Z. Phys. A – Atomic Nuclei 337, 57–69 (1990)

Zeitschrift für Physik A
Atomic Nuclei

Rapidity distributions of Ca + Ca, Nb + Nb, Ne + Au and Au + Au at bombarding energies from 250 to 2100 MeV/nucleon

H.H. Gutbrod[1], K.H. Kampert[3], B.W. Kolb[1], A.M. Poskanzer[2], H.G. Ritter[2], and H.R. Schmidt[1]

[1] Gesellschaft für Schwerionenforschung, Darmstadt, Federal Republic of Germany
[2] Lawrence Berkeley Laboratory, Berkeley, USA
[3] Institut für Kernphysik, Universität Münster, Federal Republic of Germany

Received January 30, 1990

We present experimental rapidity distributions $\mathrm{d}N_{ch}/\mathrm{d}y$ over a wide range of bombarding energies and projectile and target masses. Target and projectile spectators are observed for peripheral collisions but not for the most central collisions. This behavior is found for all systems and bombarding energies investigated. Although detector inefficiencies tend to distort the experimental distributions, they are on a tolerable level and do not remove sensitivity to theoretical descriptions.

PACS: 25.70.Np

I. Introduction

The availability of exclusive, high-statistics 4π-data [1, 2 and therein] from relativistic heavy-ion collisions and the simultaneous sophistication of non-equilibrium, nuclear transport models like the QMD [3–8, 30] or VUU/BUU apporoaches [11, 15, 27, 29, 33, 39] allow detailed, quantitative comparisons. The ultimate goal is to learn about the nuclear equation of state (EOS). Compression [36] and the resulting, experimentally verified, observables like flow angles [24] (an in-reaction-plane alignment of the transverse momenta [17, 18, 21, 29]), or the out-of-plane squeeze-out of nuclear matter [26, 34] have been suggested to be sensitively dependent on the EOS [33]. However, it has recently been pointed out [7–10, 31, 38] that the sensitivity of these observables to the EOS is distorted by the introduction of in-medium effects into the model calculations. The most important are non-local, i.e. momentum dependent interactions, and reduced in-medium $N-N$ scattering cross sections due to the Pauli-blocking of intermediate states [10 and therein]. The flow of fragments, for example, is increased both by a stiffer EOS and by momentum dependent interactions. It is, on the other hand, decreased by reduced in-medium $N-N$ cross sections.

It has been suggested that this apparent ambiguity can be resolved: if the in-medium cross section σ_{eff} entering the model calculations is reduced, then the rapidity distributions $\mathrm{d}N/\mathrm{d}y$ show effects of transparency, i.e. incomplete thermalization of the available energy. The rapidity distributions, however, do *not* depend significantly on the choice of a soft or hard EOS [7, 30]. One might thus determine σ_{eff} by comparing experimentally measured rapidity distributions and their bombarding energy dependence with model predictions.

In order to make such comparisons possible we will present experimental rapidity distributions of $Z=1$ and 2 particles measured over a wide range of bombarding energies and masses of projectile and target. Because of the wealth of the experimental data we will show as figures only a few, representative spectra. The complete set of data is contained in tables in the appendix.

II. Setup and data reduction

The experiments were performed at the Berkeley Bevalac, using the Plastic Ball/Wall spectrometer [1, 14]. This detector system has particle identification capability, in the angular range from 9 to 160° in the laboratory system, for singly and doubly charged particles as well as positively charged pions. The forward direction (0–9° in the laboratory system) is covered by the Plastic Wall, measuring time-of-flight, ΔE, and the angle of the particles, thus identifying the nuclear charge and the velocity of the particles. The rapidity variable, defined as

$$y=\frac{1}{2}\log\frac{E+p_z}{E-p_z}=\frac{1}{2}\log\frac{1+\beta_z}{1-\beta_z}$$

is therefore measured over the full angular range from 0°–160° in the laboratory for particles with charge $Z=1$ and 2. Here $E=\sqrt{p^2+m^2}$ is the total energy and p_z and β_z are the momentum and velocity components parallel to the beam axis, respectively. The inner part of the Plastic Wall (0°–2.25°) is also used to define the trigger of the whole spectrometer. The data discussed here were taken with both a minimum bias and a central collision trigger.

III. Effects of detector inefficiencies

To measure rapidity distributions dN/dy in a fixed target experiment over the full range from target to projectile rapidity is a difficult task. A large range of angles and energies contribute to a given rapidity y, e.g. midrapidity protons from a reaction at 400 MeV/nucleon have to be measured in the angular range 0° to 50° with energies larger than 80 MeV. Evidently, the experimentally measured rapidity distributions will be distorted due to detector inefficiencies. The main distortions, in the present case, result from:

i) the low energy cut-off in the Plastic Ball due to particles stopped in the target foil, the vacuum chamber or the ΔE-layer of the modules;

ii) the low velocity cut-off in the Plastic Wall;

iii) the high energy cut-off due to particles punching through the plastic scintillators. The ΔE-counters, 4 mm CaF_2 crystals, allow, to some extent, an extension of the energy measurements for punch-through particles based on the ΔE signal alone, however, at the expense of a degraded energy determination of the particles;

iv) nuclear reactions of very energetic particles in the detector modules produce a shower of reaction products causing energy leakage;

v) multiple hits in a single detector module.

Evidently, *(i)* distorts the distribution mainly at the target rapidity, while *(ii)–(iv)* are particularly disturbing in the more forward part of the Plastic Ball/Wall. Recall that at angles smaller than 9° the velocity is determined by means of time of flight in a downstream time-of-flight wall which circumvents high energy cutoffs and reaction losses to a large degree. This region is therefore predominantly distorted by effect *(v)*, which becomes increasingly import for the heavier systems and the higher bombarding energies.

As a consequence of the above detector inefficiencies the distributions will, in general, *not* be symmetric around mid rapidity as one would expect for a *AA* collision measured by an ideal detector. In order to draw quantitative conclusion from comparison with models the acceptance of the detector has therefore to be taken into account.

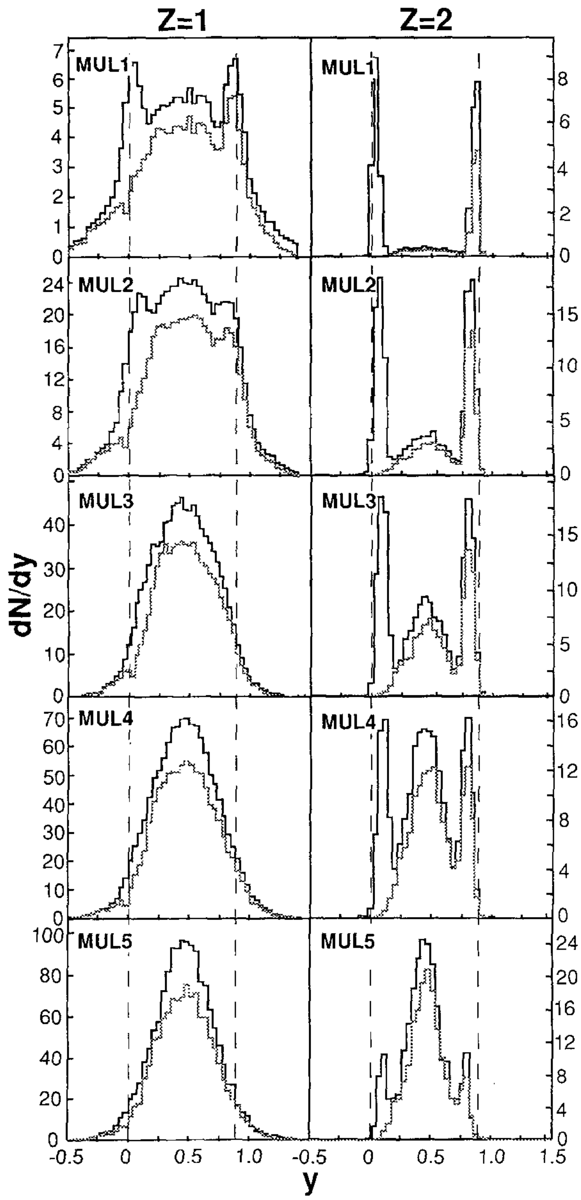

Fig. 1. FREESCO simulation results for rapidity distributions for $Z=1$ (left) and $Z=2$ (right) particles for the reaction 400 MeV/nucleon Nb+Nb grouped into five multiplicity bins. The upper solid curves are unfiltered, while the lower gray curves are the result of filtering with the Plastic Ball response. The vertical dashed lines are at target and beam rapidity

III.1. Acceptance studies with FREESCO simulations

In order to study the effect of the acceptance cuts[1] simulations have been done with the code FREESCO [22, 23] which includes collective flow of the participants [24]. The parameters, which were determined for 400 MeV/nucleon Nb+Nb, but not completely optimized, are the following. The fractional reduction in longitudinal momentum/nucleon of the spectators in the center of mass was taken to be $0.25(1-v^2)$, where v is the fraction of the maximum impact parameter. The fraction of the excitation energy leaked to the spectators was $0.05(1-v^2)$. The transverse momentum/nucleon of the spectators was $140\sqrt{4v(1-v)}$ MeV/c. The momentum/nucleon of the participant source flow was 200 MeV/c, where the tangent of the flow angle was $\sqrt{(1-v)/v}$. The results of these simulations are shown in the Fig. 1, together with a curve showing the effect of the Plastic Ball filter. The data are classified according to five multiplicity bins (MUL1–MUL5) as defined in a previous publication [17]. This selects collisions ranging from peripheral to central. The disappearance of the target rapidity peak, especially for $Z=2$ particles, is ob-

[1] Because of the complex acceptance of the Plastic Ball a FORTRAN program was written to filter the output of simulations so that they can be compared with our data. The code is available from the authors (on e-mail from POSK@LBL)

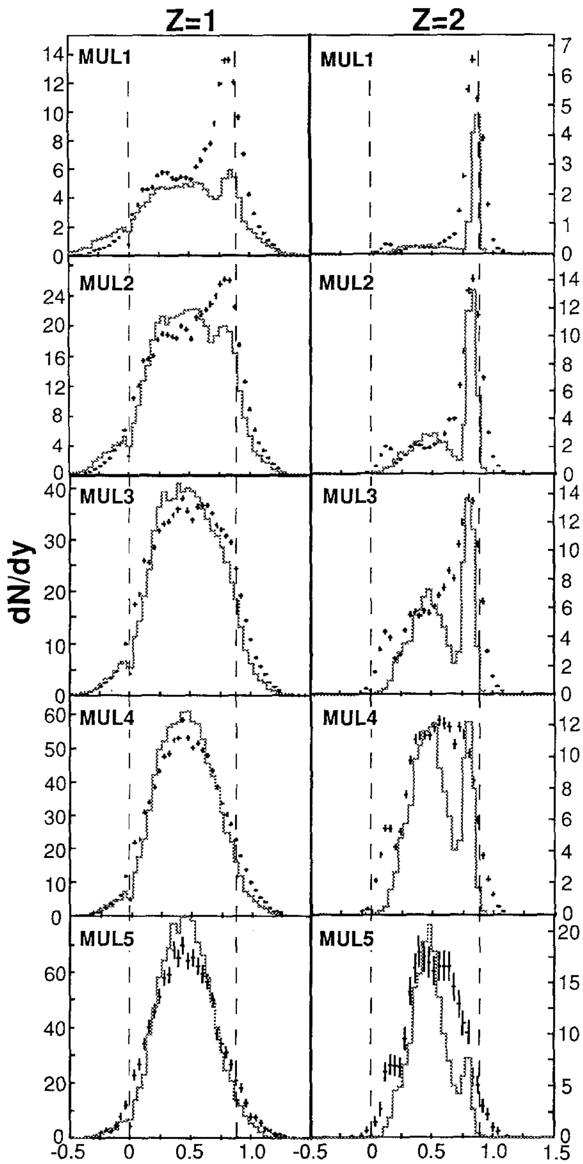

Fig. 2. Comparison of data with the FREESCO simulation for rapidity distributions for $Z=1$ (left) and $Z=2$ (right) particles for the reaction 400 MeV/nucleon Nb+Nb grouped into five multiplicity bins. The points are experimental data while the gray curves are the filtererd FREESCO results. The vertical dashed lines are at target and beam rapidity

vious, Fig. 2 shows the comparison of the filtered FREESCO results with the data. For $Z=1$ particles the simulation does not have enough of a projectile spectator peak at low multiplicities. This could probably be corrected by adjusting the parameters of FREESCO. For $Z=2$ particles the spectator and participant peaks are too well separated at medium multiplicities compared to the data. This is probably intrinsic to the three source structure of FREESCO and could not be corrected. It is hoped that simulations based on fundamental principals instead of adjustable parameters will better reproduce the data and cast light on the physics involved.

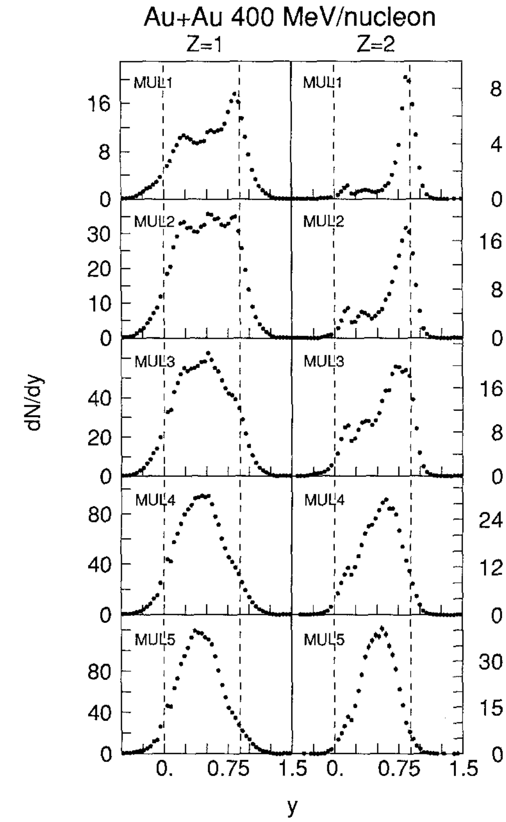

Fig. 3. Rapidity distributions of $Z=1$ (left) and $Z=2$ (right) particles from the reaction Au+Au at 400 MeV/nucleon bombarding energy. The data are classified according to five multiplicity bins. The vertical dashed lines are at target and beam rapidity

We conclude that, even though the acceptance cuts somewhat distort the experimental rapidity distributions, it should be possible to discriminate between different model descriptions.

IV. Results

Figure 3 shows, as an example, rapidity distributions for the reaction 400 MeV/nucleon Au+Au for charge $Z=1$ and 2. Values for the impact parameter range can be obtained from a comparison within the framework of the QMD model: e.g. the fifth multiplicity bin selects impact parameters $b \leqq 3$ fm [30]. As can be seen the rapidity distributions change drastically when going from very peripheral (MUL1) to the most central (MUL5) collisions: for the peripheral collision most of the charge is still located at projectile and target rapidity. The charge at target rapidity is, however, partly not detected because of absorption in the target and the detector inefficiency for low energy particles as mentioned above. For semi-central collisions (MUL2, MUL3) we observe that the projectile and target rapidity distribution begin to merge. Finally, for central collisions (MUL4, MUL5) the projectile and target distributions fully overlap, the projectile and target spectator peaks have disappeared, and the distributions are nearly gaussian shaped.

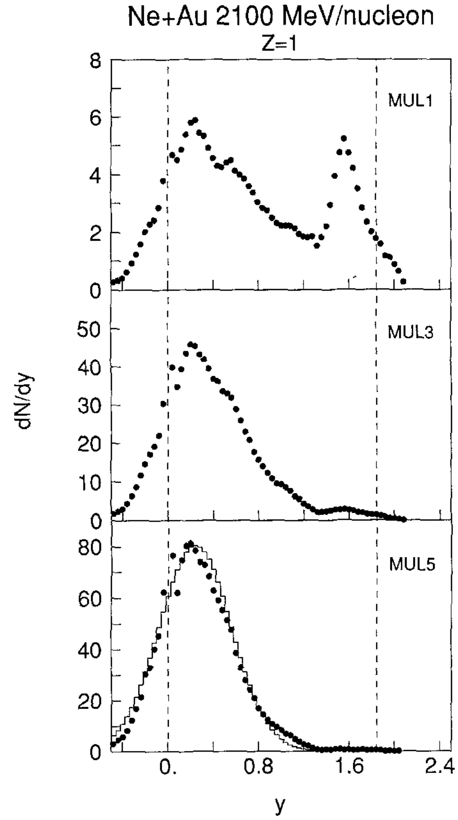

Fig. 4. Rapidity distributions of $Z=1$ particles from the reaction Ne+Au at 2100 MeV/nucleon bombarding energy selected for three different multiplicity bins. A gaussian, shown as histogram, with its center fixed at mid rapidity of the system 20 onto 197 nucleons is superimposed onto the data for the fifth multiplicity bin. The vertical dashed lines are at target and beam rapidity

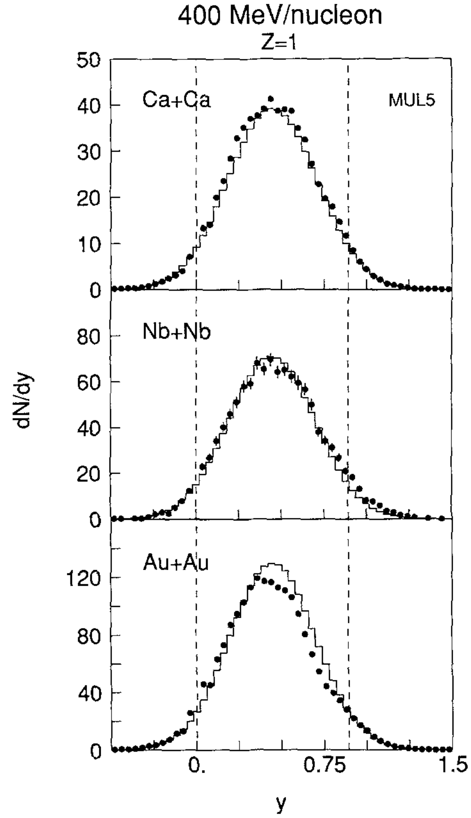

Fig. 5. Rapidity distribution for $Z=1$ particles from the reaction Ca+Ca (top), Nb+Nb (middle) and Au+Au (bottom) at 400 MeV/nucleon, selected for the fifth multiplicity bin. A gaussian (histogram) with its center fixed at mid rapidity is superimposed onto the data. The vertical dashed lines are at target and beam rapidity

The above described observations, namely the presence of spectator peaks for peripheral and their absence for central collisions demonstrate qualitatively the validity of the geometrical spectator-participant picture. For peripheral collisions only part of the projectile, predominantly in the region of geometrical overlap, is stopped while a sizeable fraction of the projectile and target remain close to their original rapidity. With increasing overlap for the more central collisions almost no remnants of projectile and target survive the collision, i.e. a mid rapidity fireball consisting of the projectile and target nucleons is formed.

Qualitatively, this behavior is observed for all projectile-target combinations at all bombarding energies under consideration. Even at the highest bombarding energy, 2100 MeV/nucleon Ne+Au, a mid rapidity fireball with practically no projectile remnants for central collisions[2] is observed as shown in Fig. 4.

Figures 5 and 6 investigate the projectile-target and bombarding energy dependence, respectively, in more detail. Figure 5 shows the rapidity distributions for 400 MeV/nucleon Ca+Ca, Nb+Nb and Au+Au for the fifth multiplicity bin. No remnants of the spectator peaks are observed for any of the systems. In the case of the lightest system, Ca+Ca, deviations from the general behavior have been reported for the average transverse energy of protons at 90° in the center of mass system [20] and for the degree of isotropy of the emission pattern [25] and had been interpreted as a sign for partial transparency. This distinction is not visible in the present representation of the data, which might be taken as an indication that the degradation of the momenta of the projectile nucleons in Ca+Ca collisions is sufficient to remove spectators, but insufficient to reach global momentum equipartition. Figure 6 shows the reaction Au+Au for 250, 400 and 650 MeV/nucleon incident energy, again for the fifth multiplicity bin. In all three cases no spectator remnants are left.

In all the MUL5 bins (Figs. 4, 5 and 6) a simple gaussian, centered at mid rapidity, is superimposed onto the data. The shape of the rapidity distributions is qualitatively reproduced by this gaussian shaped curve. In addition, detector inefficiencies are clearly visible, e.g. the apparent shift of the distribution at 650 MeV/nucleon away from midrapidity which is probably due to

[2] The upper ends of the multiplicity bins MUL1 to MUL5 for the reaction Ne+Au at 2100 MeV/nucleon are 17, 34, 51, 68 and 80, respectively

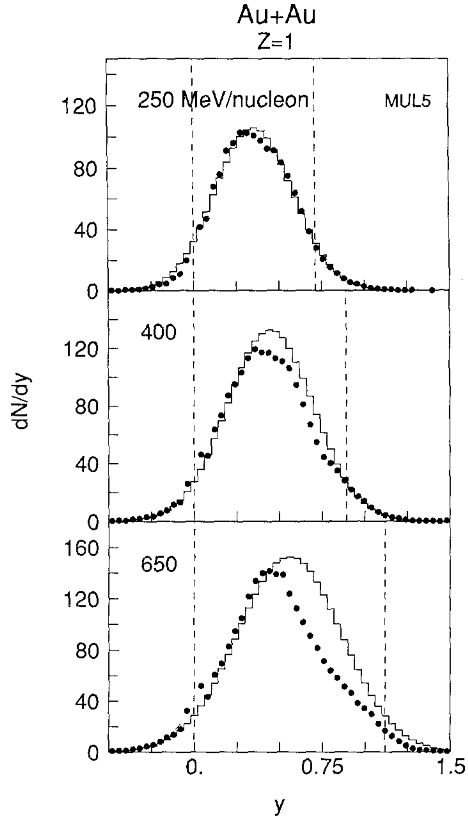

Fig. 6. Rapidity distribution for $Z=1$ particles from the reaction Au+Au at 250 (top), 400 (middle) and 650 (bottom) MeV/nucleon, selected for the fifth multiplicity bin. A gaussian (histogram) with its center fixed at mid rapidity is superimposed onto the data. The vertical dashed lines are at target and beam rapidity

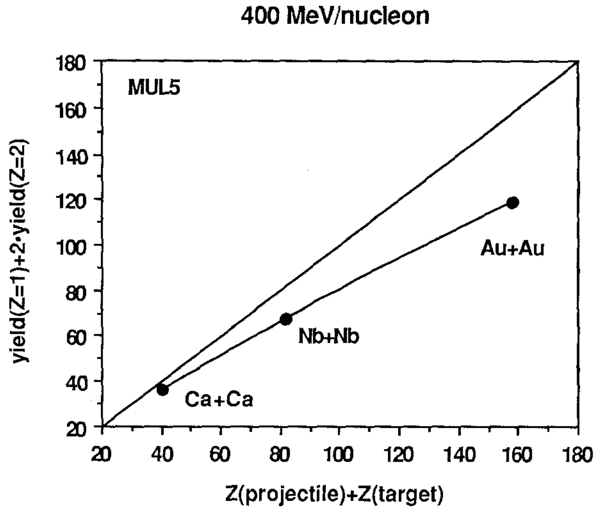

Fig. 7. Dependence of the measured summed charge of $Z=1$ and $Z=2$ particles (black circles) on the total charge of the system for 400 MeV/nucleon bombarding energy. The solid curve through the data is to guide the eye

the detector effects *(iii)–(v)* discussed above. We want to stress here again that a comparison with model predictions requires appropriate filtering of the simulated events.

This point is further illustrated in Fig. 7, where we compare the integrated charge measured for central collisions of 400 MeV/nucleon Ca+Ca, Nb+Nb and Au+Au (i.e. the integral over $Z=1$ plus twice the integral over $Z=2$ rapidity distributions for MUL5) with the total charge of the systems. The fraction of the observed charge decreases from 90% for Ca+Ca to 83% for Nb+Nb and to 75% for Au+Au. This decrease of the fraction of the observed charge is partly due to an increase in the multiple hit probability for the heavier systems. It has, however, been shown [16, 19, 28] that the fragment ratios d/p, t/p, $^{3,4}He/p$ etc. increase with the mass of the system. As a consequence a progressive fraction of the charge may be contained in intermediate mass fragments, which where, for the reactions discussed, not measured with the Plastic Ball. A comparison of a model predictions with the data should therefore be simultaneously performed for particle ratios which have been published elsewhere [16, 19].

V. Conclusions and summary

We conclude from the experimentally measured rapidity distributions a high degree of baryon stopping in central relativistic heavy-ion collision at energies ranging from 200 to 2100 MeV/nucleon. These findings are in contrast to early predictions [12, 37] of nuclear transparency at the Bevalac energy regime, but confirm qualitively predictions based on hydrodynamics [32, 35, 36].

The data presented should allow detailed comparisons with recent transport models and help to determine the in-medium $N-N$ scattering cross section σ_{eff}. The experimental distributions shown above have led theoreticians to believe that, on a qualitative level, no substantial modification of the presently employed free cross section has to be implemented into the model calculations [13, 30].

We would like to thank Prof. R. Bock for his strong support, and Dr. J. Aichelin and Prof. H. Stöcker for stimulating discussions. We acknowledge in particular the work of all present and past members of the Plastic Ball group. This work was supported in part by the U.S. Departments of Energy under Contract No. DE-AC03-76SF00098.

Appendix

Tables 1 through 8 contain the numerical values of dN_{ch}/dy for $Z=1$ and $Z=2$ particles. The graphs in Figs. 1 to 4 and the numbers in the Tables 1 to 8 are normalized to the number of events and to the unit of rapidity. The statistical error $\sigma(\mathrm{d}N_{ch}/\mathrm{d}y)$ of the data in Tables 1 to 8 can thus be obtained as $\sigma(\mathrm{d}N_{ch}/\mathrm{d}y) = \sqrt{(\mathrm{d}N_{ch}/\mathrm{d}y)/\mathrm{NF}}$. The normalization factor NF is found in Table 9.

Table 1. dN_{ch}/dy, Ca + Ca, 400 MeV/nucleon

	Z = 1					Z = 2				
y	MUL1	MUL2	MUL3	MUL4	MUL5	MUL1	MUL2	MUL3	MUL4	MUL5
−0.48		0.1	0.1	0.1	0.2					
−0.44		0.1	0.1	0.2	0.2					
−0.40		0.1	0.2	0.2	0.3					
−0.36	0.1	0.2	0.3	0.3	0.3					
−0.32	0.1	0.3	0.4	0.5	0.5					
−0.28	0.2	0.5	0.7	0.7	0.8					
−0.24	0.3	0.7	0.9	1.1	1.2					
−0.20	0.4	1.0	1.3	1.5	1.7					
−0.16	0.5	1.4	1.9	2.1	2.4					
−0.12	0.6	1.7	2.5	2.8	3.1					
−0.08	0.8	2.1	3.1	3.7	4.0			0.1	0.1	0.1
−0.04	1.1	3.0	4.8	5.9	7.1		0.1	0.1	0.1	0.2
0.04	1.9	5.1	8.5	11.3	13.3		0.3	0.6	0.9	1.1
0.08	2.1	5.7	9.2	11.9	14.0	0.1	0.6	1.4	1.9	2.2
0.12	2.8	7.7	12.7	16.8	19.9	0.2	0.9	2.0	2.7	3.1
0.16	3.2	8.8	14.7	19.9	23.5	0.1	0.7	1.6	2.4	3.4
0.20	3.7	10.1	17.3	23.6	28.3		0.3	0.9	1.6	2.3
0.24	4.0	11.3	19.2	26.4	32.7	0.1	0.4	1.1	2.2	3.3
0.28	4.1	11.5	19.8	28.0	35.1	0.1	0.6	1.6	3.0	4.6
0.32	4.2	12.0	20.5	29.3	37.0	0.1	0.8	2.0	3.8	5.8
0.36	4.2	11.9	20.5	30.0	37.7	0.1	0.8	2.1	4.1	6.3
0.40	4.2	11.8	21.2	30.8	39.2	0.1	0.7	2.0	4.0	6.1
0.44	4.7	13.2	22.9	32.6	41.2	0.1	0.6	1.9	3.8	5.4
0.48	4.6	12.9	22.0	31.4	38.7	0.1	0.7	1.9	3.8	5.8
0.52	4.8	13.4	22.4	31.6	39.0	0.1	0.8	2.1	4.1	5.9
0.56	5.3	13.9	23.0	31.4	38.6	0.1	1.0	2.5	4.5	6.3
0.60	5.5	14.2	22.4	29.4	34.9	0.3	1.4	3.3	5.4	7.1
0.64	5.9	14.9	22.2	28.2	32.4	0.3	1.7	3.7	5.3	6.8
0.68	6.8	15.1	21.1	24.8	27.2	0.7	2.8	4.9	6.0	6.8
0.72	8.9	16.7	21.0	22.5	22.8	1.7	4.9	6.7	6.5	5.9
0.76	11.9	18.5	21.0	20.9	19.7	3.7	7.9	8.6	6.8	5.2
0.80	14.2	19.0	20.3	19.1	17.8	6.9	11.0	9.6	5.9	4.0
0.84	13.2	17.1	17.6	16.1	14.6	8.2	10.6	7.9	4.3	2.5
0.88	9.8	12.7	13.0	12.2	11.7	5.5	6.4	4.6	2.4	1.4
0.92	6.3	8.4	9.1	8.8	8.5	2.6	2.9	2.1	1.1	0.7
0.96	3.7	5.4	6.0	6.0	6.0	1.3	1.1	0.8	0.5	0.4
1.00	2.2	3.5	4.0	4.2	4.4	0.4	0.4	0.3	0.2	0.1
1.04	1.4	2.2	2.7	2.9	2.9	0.1	0.1	0.1	0.1	0.1
1.08	0.8	1.5	1.8	1.9	2.2					
1.12	0.5	1.0	1.2	1.4	1.3					
1.16	0.3	0.7	0.8	0.8	0.9					
1.20	0.2	0.4	0.5	0.5	0.6					
1.24	0.1	0.2	0.3	0.3	0.3					
1.28	0.1	0.1	0.1	0.1	0.1					
1.32					0.1					

Table 2. dN_{ch}/dy, Nb + Nb, 250 MeV/nucleon

	Z = 1					Z = 2				
y	MUL1	MUL2	MUL3	MUL4	MUL5	MUL1	MUL2	MUL3	MUL4	MUL5
−0.48										
−0.44		0.1		0.1	0.1					
−0.40	0.1	0.1	0.1	0.2	0.1					
−0.36	0.1	0.1	0.2	0.3	0.5					
−0.32	0.1	0.3	0.5	0.6	0.6					
−0.28	0.2	0.6	0.9	0.8	0.5					
−0.24	0.4	0.9	1.1	1.3	1.3					
−0.20	0.5	1.4	1.8	1.8	2.2					
−0.16	0.6	1.9	2.6	2.9	3.3					

Table 2 (continued)

y	$Z=1$ MUL1	MUL2	MUL3	MUL4	MUL5	$Z=2$ MUL1	MUL2	MUL3	MUL4	MUL5
−0.12	0.8	2.4	3.7	4.1	4.6					0.2
−0.08	1.1	3.3	5.2	5.7	6.5		0.1	0.1	0.2	0.1
−0.04	1.5	4.9	7.9	9.9	10.6		0.1	0.4	0.6	0.3
0.04	2.6	8.6	14.7	20.3	23.3	0.1	0.7	1.9	2.8	3.0
0.08	3.3	11.1	17.9	23.5	27.1	0.2	1.4	3.8	5.7	6.7
0.12	4.0	14.2	25.0	31.8	37.9	0.4	2.5	5.6	8.2	10.2
0.16	4.7	16.5	28.5	37.4	44.8	0.4	2.0	4.7	7.8	10.2
0.20	5.5	19.0	32.7	44.6	51.9	0.1	0.9	2.7	4.8	7.8
0.24	5.9	19.8	35.0	45.6	56.3	0.1	1.3	3.4	6.7	9.3
0.28	6.0	19.9	34.8	48.4	60.4	0.2	1.5	4.2	8.1	12.5
0.32	6.1	19.8	34.1	49.5	60.5	0.2	1.9	5.3	9.9	14.9
0.36	5.8	19.5	33.6	49.2	63.0	0.3	2.1	5.9	12.0	18.2
0.40	6.0	19.8	34.3	50.1	60.4	0.3	2.3	6.1	12.1	19.3
0.44	6.6	20.6	35.7	47.8	58.5	0.4	2.5	7.1	12.7	19.1
0.48	6.9	21.8	37.0	49.6	60.3	0.5	3.4	7.7	13.6	19.8
0.52	8.5	25.0	40.1	51.6	57.9	0.9	4.3	9.0	13.8	17.1
0.56	10.6	27.1	40.8	49.6	55.8	1.5	6.3	11.1	15.1	18.1
0.60	12.3	29.4	39.3	45.6	49.1	2.8	9.7	14.9	15.9	16.9
0.64	14.5	30.8	38.2	40.8	39.8	5.6	14.6	18.1	16.6	14.9
0.68	13.5	26.1	30.3	30.5	28.1	7.0	17.0	19.1	15.1	13.1
0.72	11.7	21.6	23.7	22.5	20.7	6.2	14.6	15.2	12.0	9.5
0.76	9.8	16.8	17.7	16.7	16.2	4.4	8.9	9.1	6.8	6.0
0.80	7.1	11.8	11.9	11.5	11.9	1.8	3.6	4.1	3.5	3.1
0.84	4.4	7.8	8.7	8.4	8.1	0.4	1.3	1.8	1.9	2.1
0.88	2.5	5.0	5.8	5.7	6.8	0.1	0.6	1.1	1.1	1.5
0.92	1.6	3.3	3.9	4.2	4.2	0.1	0.5	0.8	0.9	1.0
0.96	1.1	2.3	2.7	2.7	2.3	0.1	0.3	0.5	0.5	0.9
1.00	0.8	1.6	1.8	1.9	1.6		0.2	0.2	0.2	0.3
1.04	0.5	1.2	1.3	1.4	1.2					0.1
1.08	0.4	0.8	1.0	1.0	1.0					
1.12	0.3	0.6	0.7	0.7	0.5					
1.16	0.2	0.4	0.5	0.5	0.3					
1.20	0.2	0.3	0.3	0.3	0.2					
1.24	0.1	0.2	0.2	0.3	0.1					
1.28	0.1	0.1	0.1	0.2	0.2					

Table 3. dN_{ch}/dy, Nb + Nb, 400 MeV/nucleon

y	$Z=1$ MUL1	MUL2	MUL3	MUL4	MUL5	$Z=2$ MUL1	MUL2	MUL3	MUL4	MUL5
−0.48		0.1	0.1	0.1						
−0.44		0.1	0.1	0.1						
−0.40	0.1	0.2	0.2	0.3						
−0.36	0.1	0.3	0.4	0.4	0.5					
−0.32	0.2	0.5	0.7	0.7	0.3					
−0.28	0.4	0.9	1.3	1.1	0.9					
−0.24	0.5	1.2	1.7	1.5	2.1					
−0.20	0.5	1.7	2.5	2.3	2.9					
−0.16	0.7	2.3	3.3	3.7	2.5					
−0.12	1.0	3.4	4.6	4.7	5.0		0.1	0.1	0.1	
−0.08	1.3	4.2	6.2	6.2	7.9		0.1	0.2	0.2	0.2
−0.04	1.7	6.1	9.9	11.7	12.3		0.1	0.4	0.4	0.7
0.04	2.9	10.4	17.5	21.9	22.9	0.1	0.6	1.6	2.1	1.5
0.08	3.5	12.1	19.4	22.9	26.9	0.2	1.4	3.1	3.7	2.8
0.12	4.6	15.4	25.8	31.0	34.1	0.4	2.0	4.3	5.4	6.4
0.16	4.6	15.6	25.5	34.1	40.2	0.3	1.8	3.9	5.4	7.1
0.20	4.8	16.1	28.5	38.5	45.8	0.1	0.8	2.5	4.3	6.9
0.24	5.6	18.2	31.7	43.4	51.2	0.1	1.0	2.8	5.2	6.8
0.28	5.8	19.0	33.1	47.7	58.0	0.2	1.4	4.4	7.6	9.6

Table 3 (continued)

	Z=1					Z=2				
y	MUL1	MUL2	MUL3	MUL4	MUL5	MUL1	MUL2	MUL3	MUL4	MUL5
0.32	5.8	18.9	33.6	48.6	59.1	0.3	2.0	5.5	9.7	14.1
0.36	5.4	18.7	34.9	52.5	68.2	0.3	2.2	5.7	11.1	16.4
0.40	5.3	18.5	36.0	53.2	65.5	0.2	2.1	5.4	11.3	18.1
0.44	5.5	20.0	38.1	58.6	69.9	0.2	1.9	5.8	11.3	17.6
0.48	5.4	19.5	35.6	53.2	64.4	0.2	2.0	5.6	11.3	17.0
0.52	5.3	18.3	33.8	50.2	65.3	0.2	2.2	6.1	11.8	16.2
0.56	6.2	21.1	36.4	51.6	62.3	0.4	2.4	6.9	12.3	16.7
0.60	6.8	21.6	36.5	49.8	59.4	0.5	3.2	7.8	12.1	16.5
0.64	7.4	22.2	36.6	47.9	56.7	0.6	3.9	8.6	11.8	16.7
0.68	7.8	22.9	35.2	43.7	50.0	0.7	4.0	8.0	10.7	14.6
0.72	9.3	24.0	32.9	38.5	38.1	1.5	6.4	10.4	11.9	13.0
0.76	11.9	25.6	32.1	33.9	34.1	2.6	8.9	12.0	11.4	11.1
0.80	13.6	26.1	30.7	30.4	31.1	5.6	13.2	13.7	10.2	10.2
0.84	13.6	26.0	29.5	27.6	26.7	6.6	14.1	13.5	8.5	5.9
0.88	12.1	22.5	24.4	22.7	20.8	5.2	11.5	10.5	6.0	5.1
0.92	9.7	17.6	19.1	17.8	18.2	3.9	7.0	6.4	3.7	3.1
0.96	7.1	12.6	14.4	13.6	13.0	1.7	3.0	3.0	2.2	2.3
1.00	4.3	8.9	10.7	10.0	8.0	0.5	1.2	1.3	1.3	1.0
1.04	2.9	6.2	7.3	7.7	7.6	0.2	0.6	0.6	0.5	0.6
1.08	2.0	4.5	5.6	5.6	5.8	0.1	0.2	0.3	0.2	
1.12	1.5	3.5	4.1	4.3	3.5		0.1	0.1		
1.16	1.0	2.4	2.6	2.5	2.8					
1.20	0.8	1.5	1.7	1.6	1.6					
1.24	0.4	1.0	1.0	1.1	1.3					
1.28	0.2	0.4	0.4	0.4	0.8					

Table 4. dN_{ch}/dy, Nb + Nb, 650 MeV/nucleon

	Z=1					Z=2				
y	MUL1	MUL2	MUL3	MUL4	MUL5	MUL1	MUL2	MUL3	MUL4	MUL5
−0.48		0.1	0.4	0.5	0.6					
−0.44	0.1	0.2	0.5	0.5	0.2					
−0.40	0.2	0.3	0.6	0.5	0.8					
−0.36	0.2	0.7	1.0	0.8	0.8					
−0.32	0.4	0.9	1.4	1.2	0.4					
−0.28	0.5	1.4	1.9	1.6	1.8					
−0.24	0.7	2.1	2.7	2.5	2.2					
−0.20	0.9	2.6	3.5	3.4	4.6				0.1	
−0.16	1.5	3.5	4.9	4.8	4.8			0.1	0.1	
−0.12	1.5	4.6	6.3	6.6	5.2		0.1	0.1	0.2	
−0.08	2.1	5.9	8.2	9.1	8.9		0.2	0.4	0.4	0.4
−0.04	2.5	8.3	13.4	14.5	20.4		0.3	0.6	0.8	1.0
0.04	4.1	13.0	19.9	24.8	28.0	0.1	0.8	1.7	1.7	2.4
0.08	4.5	13.2	20.2	22.0	24.6	0.2	1.6	2.6	2.8	3.4
0.12	5.6	16.2	24.1	27.1	28.8	0.4	2.0	3.3	4.0	3.2
0.16	5.2	16.6	25.6	32.4	38.1	0.4	1.5	3.4	3.7	4.2
0.20	5.5	17.3	27.0	35.3	42.3	0.1	0.8	2.0	3.1	3.0
0.24	6.1	17.0	28.6	39.4	50.4	0.1	0.8	2.4	2.9	4.2
0.28	6.2	18.9	30.2	43.2	54.2	0.1	1.1	3.2	4.2	5.8
0.32	5.8	17.7	32.1	49.1	65.7	0.2	1.5	3.4	5.6	10.9
0.36	5.2	18.0	33.1	50.7	64.9	0.2	1.5	4.4	6.8	10.1
0.40	5.3	17.2	32.6	54.3	67.7	0.2	1.5	3.6	6.4	8.9
0.44	5.5	17.9	35.2	59.7	67.9	0.1	1.2	3.2	6.7	10.3
0.48	5.1	17.3	34.3	56.5	73.2	0.1	1.0	3.0	6.6	6.8
0.52	4.9	17.0	33.0	52.7	63.5	0.1	1.1	3.0	7.1	10.3
0.56	5.6	18.4	34.3	56.1	67.5	0.1	1.0	3.2	6.8	8.3
0.60	6.0	18.5	35.8	52.9	66.5	0.1	1.1	3.7	7.5	9.7
0.64	6.1	19.0	34.4	49.4	66.1	0.1	1.1	3.7	8.3	12.7
0.68	6.2	18.1	32.8	47.9	58.9	0.2	1.3	3.8	7.7	11.3

Table 4 (continued)

	$Z=1$					$Z=2$				
y	MUL1	MUL2	MUL3	MUL4	MUL5	MUL1	MUL2	MUL3	MUL4	MUL5
0.72	5.9	17.4	30.8	44.4	55.0	0.3	1.8	4.3	8.5	12.7
0.76	6.1	16.3	27.9	40.2	51.2	0.3	2.1	5.2	7.9	11.7
0.80	6.1	17.8	28.2	36.8	43.7	0.3	2.4	5.3	8.3	9.9
0.84	6.4	19.0	28.2	36.3	42.1	0.4	2.8	4.7	7.6	7.7
0.88	8.2	20.6	28.5	35.3	34.5	0.7	3.3	5.9	6.4	9.7
0.92	10.1	23.3	30.0	31.5	35.7	1.4	4.4	6.1	5.9	6.2
0.96	13.7	24.5	30.9	30.9	31.0	2.5	6.8	7.7	5.5	4.2
1.00	16.8	27.8	31.3	29.5	29.0	4.4	9.7	9.5	5.6	4.2
1.04	16.6	27.2	29.8	26.0	21.4	6.3	11.0	10.5	5.0	3.8
1.08	15.0	24.1	26.6	22.2	19.8	6.5	12.1	9.9	4.3	2.8
1.12	12.6	19.8	20.5	18.2	16.3	5.8	9.7	7.4	2.9	1.8
1.16	9.1	14.0	15.7	13.4	10.3	3.8	5.7	4.6	1.9	0.4
1.20	6.3	9.9	10.1	9.0	7.3	2.0	2.7	2.4	1.0	0.4
1.24	3.7	5.9	6.5	6.0	5.6	0.8	1.2	1.0	0.7	0.4
1.28	2.3	3.3	4.0	3.5	3.0	0.3	0.7	0.5	0.3	0.2
1.32	0.7	1.4	1.3	1.3	1.0	0.1	0.3	0.2	0.2	0.2
1.36	0.5	0.8	1.0	0.5	0.6		0.1	0.1	0.1	0.2
1.40	0.3	0.6	0.6	0.5	0.4			0.1		
1.44	0.2	0.4	0.4	0.6	0.6					
1.48	0.1	0.3	0.3	0.5	1.0					

Table 5. dN_{ch}/dy, Au + Au, 250 MeV/nucleon

	$Z=1$					$Z=2$				
y	MUL1	MUL2	MUL3	MUL4	MUL5	MUL1	MUL2	MUL3	MUL4	MUL5
−0.48			0.1	0.1	0.2					
−0.44	0.1	0.1	0.1	0.1	0.1					
−0.40	0.1	0.1	0.1	0.2	0.4					
−0.36	0.1	0.2	0.4	0.4	0.4					
−0.32	0.3	0.6	0.8	1.0	0.8				0.1	
−0.28	0.4	1.2	1.7	1.7	1.4				0.3	
−0.24	0.6	1.7	2.4	2.9	2.4				0.8	
−0.20	0.8	2.6	3.9	4.2	4.1				0.6	
−0.16	1.0	3.7	5.3	6.0	4.7			0.1	0.8	
−0.12	1.3	4.7	7.3	9.5	8.5		0.1	0.2	0.9	0.1
−0.08	1.7	6.1	9.9	12.4	11.0		0.2	0.4	1.2	0.5
−0.04	2.1	8.4	14.4	19.4	19.7		0.3	0.7	2.0	0.7
0.04	3.6	14.0	25.4	35.6	41.7	0.2	1.2	3.3	5.1	5.3
0.08	4.7	18.4	30.3	41.1	47.1	0.4	2.8	6.5	9.6	10.9
0.12	6.2	23.7	40.3	56.4	67.7	0.7	4.9	10.0	14.0	16.3
0.16	7.4	28.2	46.8	64.4	75.9	1.0	6.1	11.8	17.8	23.2
0.20	8.5	33.2	54.0	74.6	91.5	0.4	2.8	7.1	13.6	18.4
0.24	9.3	34.7	57.0	79.8	96.2	0.3	3.0	7.9	15.4	23.9
0.28	9.1	33.3	56.2	81.0	103.0	0.5	4.2	11.1	20.0	30.1
0.32	8.9	32.2	55.0	82.0	102.0	0.6	5.2	12.6	24.5	34.6
0.36	8.4	31.4	54.8	80.7	101.0	0.7	5.5	13.9	27.1	41.4
0.40	8.6	31.8	54.9	80.2	97.8	0.7	5.1	13.7	27.4	41.8
0.44	9.1	33.1	54.3	77.2	92.4	0.8	5.6	13.0	26.2	38.4
0.48	9.5	34.0	55.9	75.8	91.5	0.9	6.5	14.8	27.5	39.6
0.52	10.7	37.1	57.3	75.5	83.8	1.5	8.6	17.4	27.1	36.5
0.56	12.1	38.4	55.8	69.5	74.9	2.1	10.9	20.4	27.2	34.3
0.60	13.4	39.2	51.5	59.0	63.5	4.0	15.8	23.7	28.8	31.6
0.64	14.6	38.8	48.5	52.2	51.8	6.5	19.8	25.9	26.2	26.9
0.68	12.9	32.7	39.4	39.1	38.6	6.6	21.0	26.4	23.7	21.3
0.72	10.8	26.4	30.8	30.1	28.0	5.3	17.9	22.0	19.1	16.4
0.76	9.0	21.1	24.3	22.2	20.6	4.7	13.4	15.6	12.6	10.7
0.80	7.4	16.3	17.9	16.2	15.0	3.2	7.8	8.4	6.6	6.0
0.84	5.3	11.4	12.1	11.4	11.3	1.2	3.4	4.0	4.5	3.5
0.88	3.5	7.4	8.2	8.1	7.9	0.4	1.5	2.3	2.7	2.7

Table 5 (continued)

	$Z=1$					$Z=2$				
y	MUL1	MUL2	MUL3	MUL4	MUL5	MUL1	MUL2	MUL3	MUL4	MUL5
0.92	2.2	4.6	5.2	5.2	5.4	0.2	0.9	1.5	1.7	2.3
0.96	1.5	3.0	3.5	3.6	4.1	0.1	0.5	0.8	1.0	0.8
1.00	0.9	2.2	2.3	2.5	2.6	0.1	0.3	0.4	0.4	0.2
1.04	0.7	1.4	1.5	1.6	1.5		0.1	0.1	0.1	0.1
1.08	0.4	0.9	1.1	1.2	1.2					
1.12	0.3	0.7	0.8	0.8	0.5					
1.16	0.3	0.4	0.5	0.5	0.4					
1.20	0.2	0.3	0.3	0.3	0.1					
1.24	0.1	0.2	0.2	0.2	0.2					
1.28	0.1	0.1	0.1	0.1	0.1					

Table 6. dN_{ch}/dy, Au + Au, 400 MeV/nucleon

	$Z=1$					$Z=2$				
y	MUL1	MUL2	MUL3	MUL4	MUL5	MUL1	MUL2	MUL3	MUL4	MUL5
−0.48	0.1	0.2	0.2	0.4	0.2					
−0.44	0.1	0.2	0.3	0.4	0.6					
−0.40	0.2	0.4	0.5	0.5	0.6					
−0.36	0.3	0.6	0.9	0.9	1.2					
−0.32	0.5	1.4	1.7	1.8	1.7			0.1		
−0.28	0.9	2.2	3.0	2.8	2.9			0.3	0.1	
−0.24	1.3	2.9	4.3	4.3	3.4			0.5	0.2	
−0.20	1.7	4.2	6.5	6.4	5.3			0.5	0.2	
−0.16	1.9	5.3	8.5	8.6	7.5		0.1	0.7	0.4	0.1
−0.12	2.4	7.1	11.7	12.5	11.6		0.2	0.8	0.7	0.2
−0.08	2.8	8.7	14.0	15.2	13.2	0.1	0.4	1.2	0.9	0.8
−0.04	3.7	11.8	19.8	25.0	25.9	0.1	0.5	1.9	1.9	1.3
0.04	5.6	18.4	32.7	43.6	46.2	0.3	1.6	4.1	5.3	4.5
0.08	6.4	20.5	33.8	42.1	45.5	0.5	2.8	6.8	7.9	6.6
0.12	8.1	26.0	42.9	57.5	63.4	0.8	4.4	8.9	10.1	8.9
0.16	9.1	29.2	47.5	64.2	73.2	1.0	4.9	9.2	11.7	11.9
0.20	10.3	33.0	52.0	72.1	87.3	0.4	2.6	6.4	10.0	10.8
0.24	10.7	33.4	55.1	79.6	95.1	0.4	2.7	6.9	11.9	15.5
0.28	10.3	31.7	53.5	83.6	103.0	0.5	3.5	8.5	14.7	20.4
0.32	10.0	31.7	54.5	87.1	113.0	0.6	4.3	9.8	17.6	25.6
0.36	9.5	30.5	55.0	92.2	119.0	0.6	4.0	10.0	20.5	31.4
0.40	9.4	30.5	56.0	93.0	117.0	0.6	3.7	9.9	22.2	34.6
0.44	9.6	31.9	58.0	94.2	117.0	0.5	3.1	9.3	22.6	36.6
0.48	9.7	32.5	58.3	93.2	113.0	0.5	3.6	10.1	24.2	38.3
0.52	11.2	35.7	62.6	94.1	111.0	0.6	4.2	11.4	26.3	37.9
0.56	11.5	35.5	59.2	87.6	106.0	0.6	4.7	13.7	28.2	40.5
0.60	11.2	34.2	55.1	77.7	94.5	0.9	6.3	15.5	29.0	38.6
0.64	11.5	34.5	53.3	71.3	80.8	1.1	7.3	15.6	26.7	34.9
0.68	11.7	32.6	48.8	60.3	66.7	1.7	9.3	18.6	26.8	32.1
0.72	12.6	32.3	44.9	52.7	54.7	2.7	11.6	19.9	25.3	27.4
0.76	14.6	33.0	42.2	45.5	44.4	4.0	13.6	19.8	21.2	20.8
0.80	16.3	34.6	41.4	41.9	40.0	6.6	16.1	19.0	17.1	15.7
0.84	17.5	34.9	39.1	37.4	34.9	8.8	18.2	19.3	13.6	10.1
0.88	16.2	30.6	34.6	32.0	28.2	8.5	17.5	18.1	11.0	7.2
0.92	13.5	25.7	28.8	25.6	22.0	6.8	13.9	13.9	7.8	4.8
0.96	10.4	19.5	21.6	19.2	17.1	4.7	8.7	8.6	4.7	2.6
1.00	7.5	13.9	15.3	13.7	13.8	2.3	4.4	4.3	2.5	1.6
1.04	4.8	8.9	10.6	9.7	9.3	0.9	1.5	1.8	1.0	0.4
1.08	3.3	5.9	6.8	6.5	6.3	0.3	0.7	0.7	0.4	0.3
1.12	2.1	3.9	4.3	4.3	4.1	0.1	0.2	0.3	0.2	0.1
1.16	1.4	2.7	2.9	2.9	2.5		0.1	0.1	0.1	0.1
1.20	0.9	1.7	1.9	1.8	1.9			0.1	0.1	
1.24	0.6	1.0	1.0	0.9	1.1					

Table 6 (continued)

y	$Z=1$ MUL1	MUL2	MUL3	MUL4	MUL5	$Z=2$ MUL1	MUL2	MUL3	MUL4	MUL5
1.28	0.3	0.5	0.5	0.5	0.5					
1.32		0.1	0.2	0.1						
1.36		0.1	0.1	0.2	0.1					
1.40		0.1	0.1	0.1	0.1					
1.44		0.1	0.1	0.1	0.1					
1.48			0.1	0.1	0.1					

Table 7. dN_{ch}/dy, Au + Au, 650 MeV/nucleon

y	$Z=1$ MUL1	MUL2	MUL3	MUL4	MUL5	$Z=2$ MUL1	MUL2	MUL3	MUL4	MUL5
−0.48	0.3	0.4	0.6	0.8	0.9					
−0.44	0.3	0.5	0.8	1.1	1.2					
−0.40	0.4	0.7	1.2	1.4	1.5					
−0.36	0.7	1.3	1.9	2.1	2.2					
−0.32	1.1	2.2	3.1	3.4	2.9					
−0.28	1.6	3.1	4.5	4.7	4.5					
−0.24	2.2	4.7	6.5	6.7	5.9			0.1		
−0.20	3.0	5.8	9.3	9.4	8.5			0.1	0.1	0.1
−0.16	3.5	7.6	11.7	12.4	11.5		0.1	0.3	0.3	0.2
−0.12	4.2	9.3	14.8	16.3	13.8	0.1	0.3	0.6	0.6	0.3
−0.08	4.8	11.0	17.3	19.8	18.1	0.1	0.5	1.1	1.1	0.7
−0.04	6.6	15.5	25.8	32.6	32.6	0.2	0.7	1.7	2.0	1.5
0.04	9.4	21.5	37.0	49.3	52.1	0.4	1.8	3.9	4.8	3.6
0.08	9.6	21.9	34.4	43.2	43.5	0.8	2.9	5.7	6.0	4.6
0.12	11.9	26.9	43.5	55.9	61.0	1.1	3.6	6.7	7.2	5.4
0.16	13.1	29.2	46.4	62.0	69.4	1.2	3.6	6.4	7.8	7.3
0.20	13.9	31.8	51.0	70.0	82.8	0.5	2.0	4.7	7.5	7.9
0.24	14.4	32.5	53.0	76.9	94.7	0.5	2.3	5.3	8.2	9.4
0.28	13.9	31.3	53.0	82.8	105.0	0.6	2.8	6.2	10.0	13.0
0.32	13.0	30.2	54.6	91.1	121.0	0.8	2.9	7.0	12.5	16.5
0.36	12.8	30.6	56.7	99.0	134.0	0.7	3.1	7.3	14.3	19.4
0.40	12.3	30.8	58.4	105.0	140.0	0.7	2.7	7.3	16.2	23.7
0.44	12.3	31.0	60.8	110.0	142.0	0.6	2.4	6.7	17.0	26.8
0.48	12.2	31.5	62.2	108.0	139.0	0.4	2.3	7.0	19.1	31.0
0.52	13.6	35.0	66.5	111.0	138.0	0.4	2.4	7.9	20.6	32.5
0.56	13.9	34.1	62.6	102.0	124.0	0.5	2.6	8.6	22.4	34.5
0.60	12.9	31.4	56.5	91.4	113.0	0.5	3.1	9.3	22.6	34.6
0.64	13.2	31.1	54.2	84.7	101.0	0.6	3.1	9.2	21.6	32.8
0.68	13.0	29.0	51.4	76.2	90.9	0.8	4.0	11.3	23.5	33.3
0.72	12.4	27.8	47.7	68.8	81.6	1.2	5.0	12.8	24.7	32.8
0.76	12.4	27.7	45.1	61.6	71.5	1.3	5.6	13.0	21.8	26.8
0.80	13.1	28.4	43.2	57.0	64.2	1.4	5.4	11.7	17.4	19.3
0.84	14.0	28.9	43.9	54.2	58.2	1.7	5.7	10.7	14.3	15.3
0.88	16.1	31.5	43.7	50.5	51.3	2.2	6.5	10.7	12.2	12.3
0.92	19.3	33.8	45.2	47.0	46.5	3.6	8.4	11.7	10.3	8.0
0.96	23.1	37.7	45.5	44.0	38.5	6.7	11.9	14.0	9.5	5.8
1.00	26.6	39.5	44.7	40.6	34.1	10.3	15.9	16.1	8.9	4.5
1.04	26.4	37.2	41.5	35.4	29.6	11.8	17.2	16.6	8.5	3.0
1.08	21.9	31.3	33.9	28.4	22.1	10.5	14.9	14.6	7.5	2.9
1.12	17.2	24.0	26.1	21.3	16.8	7.7	11.0	10.9	5.4	2.1
1.16	12.6	17.4	18.4	15.1	12.6	4.6	7.0	6.8	3.5	1.2
1.20	8.5	11.8	12.5	10.3	8.4	2.8	4.1	4.1	2.1	0.8
1.24	5.3	7.7	7.7	6.7	5.2	1.3	2.0	2.1	1.3	0.5
1.28	3.1	4.6	4.7	3.9	3.0	0.6	1.0	1.1	0.7	0.4
1.32	1.5	2.2	2.4	2.1	1.8	0.4	0.6	0.6	0.5	0.2
1.36	0.9	1.4	1.7	1.6	1.5	0.2	0.3	0.4	0.3	0.1
1.40	0.5	0.9	1.1	1.1	1.1	0.1	0.2	0.2	0.2	0.1
1.44	0.4	0.7	0.9	0.9	0.9	0.1	0.1	0.2	0.1	0.1
1.48	0.3	0.5	0.7	0.7	0.8		0.1	0.1	0.1	0.1

Table 8. dN_{ch}/dy, Ne + Au, 2100 MeV/nucleon

	$Z=1$					$Z=2$				
y	MUL1	MUL2	MUL3	MUL4	MUL5	MUL1	MUL2	MUL3	MUL4	MUL5
−0.48	0.3	0.8	1.7	2.7	3.1					
−0.44	0.3	1.2	2.3	3.5	4.6					
−0.40	0.4	1.5	2.9	4.5	5.7					
−0.36	0.6	2.3	4.3	6.4	8.2					0.1
−0.32	0.9	3.4	6.3	9.5	12.2				0.1	0.9
−0.28	1.2	4.9	8.6	12.7	16.8			0.1	0.1	2.2
−0.24	1.6	6.3	11.6	16.4	21.3				0.2	4.0
−0.20	2.0	7.8	14.5	21.3	30.3			0.1	0.3	3.5
−0.16	2.3	9.4	17.1	25.0	32.9		0.1	0.3	0.7	5.0
−0.12	2.4	10.3	19.2	28.2	40.1		0.2	0.6	1.1	4.1
−0.08	2.8	11.9	22.0	33.1	45.4	0.1	0.3	0.8	1.6	5.5
−0.04	3.8	16.0	30.3	46.5	62.2	0.1	0.4	1.1	2.2	8.3
0.04	4.7	20.8	39.8	61.6	76.5	0.1	0.8	2.1	4.0	6.1
0.08	4.5	18.6	34.6	51.8	62.0	0.2	1.1	2.6	4.8	7.3
0.12	4.9	20.8	39.2	59.3	74.7	0.2	1.5	3.5	5.5	7.9
0.16	5.4	23.5	43.4	64.5	80.4	0.2	1.6	3.5	5.9	8.2
0.20	5.8	24.5	45.9	67.7	81.2	0.1	0.8	2.0	4.2	6.3
0.24	5.9	24.2	45.4	66.4	78.6	0.1	0.8	2.1	4.1	6.6
0.28	5.4	22.9	43.2	63.4	74.0	0.1	0.9	2.6	5.0	6.0
0.32	5.3	21.9	41.9	61.7	72.8	0.1	1.0	3.0	5.2	7.9
0.36	4.9	20.6	39.5	58.6	68.3	0.1	0.9	2.6	4.4	6.2
0.40	4.6	19.2	36.7	54.2	62.8	0.1	0.7	2.2	4.2	5.8
0.44	4.3	18.5	36.2	51.7	59.1	0.1	0.6	1.5	3.2	4.5
0.48	4.3	17.8	33.6	47.1	55.3		0.4	1.4	2.9	4.7
0.52	4.4	17.9	33.0	45.1	51.5		0.4	1.3	2.7	3.8
0.56	4.5	17.6	31.9	41.6	47.7		0.3	1.2	2.6	3.5
0.60	4.1	16.1	28.8	36.5	38.6		0.4	1.1	2.3	3.0
0.64	4.0	15.2	25.9	32.5	32.9		0.3	1.0	1.8	2.6
0.68	3.9	13.8	22.9	28.1	27.9		0.3	1.0	1.7	2.6
0.72	3.6	12.9	20.7	23.8	24.2	0.1	0.3	0.9	1.7	2.1
0.76	3.4	11.3	17.7	20.1	21.0		0.3	0.7	1.0	1.2
0.80	3.0	10.3	15.7	16.9	16.9		0.2	0.4	0.7	0.9
0.84	2.8	9.4	14.0	15.4	14.5		0.1	0.3	0.5	0.5
0.88	2.8	8.6	12.3	13.1	12.3		0.1	0.3	0.3	0.4
0.92	2.5	7.7	10.8	11.4	10.8		0.1	0.2	0.2	0.3
0.96	2.3	7.1	9.5	10.1	9.5		0.1	0.1	0.2	0.3
1.00	2.2	6.8	9.3	9.1	8.4		0.1	0.1	0.1	0.1
1.04	2.2	6.5	8.6	8.3	7.0		0.1	0.1	0.1	0.1
1.08	2.2	6.1	7.6	6.7	6.4		0.1	0.1	0.1	
1.12	2.1	5.3	6.2	5.5	4.9		0.1	0.1	0.1	
1.16	1.9	4.8	5.4	4.4	3.8		0.1	0.1	0.1	0.1
1.20	1.9	4.3	4.2	3.6	2.8	0.1	0.1	0.1	0.1	0.1
1.24	1.8	3.7	3.5	2.6	2.3	0.1	0.1	0.1	0.1	
1.28	1.9	3.3	2.7	1.9	1.4	0.1	0.1	0.1	0.1	
1.32	1.5	2.7	2.0	1.3	0.9	0.2	0.2	0.1	0.1	0.1
1.36	1.8	3.0	2.2	1.2	0.6	0.2	0.2	0.1	0.1	
1.40	2.2	3.3	2.2	1.2	0.7	0.2	0.2	0.1		
1.44	2.9	3.9	2.4	1.1	0.6	0.3	0.3	0.1		
1.48	3.9	4.3	2.7	1.1	0.9	0.4	0.5	0.1		
1.52	4.8	5.0	2.6	1.2	0.8	0.8	0.7	0.2	0.1	
1.56	5.2	5.3	2.8	1.2	0.4	1.6	1.1	0.3	0.1	
1.60	4.7	4.8	2.5	1.1	0.7	2.0	1.2	0.2		
1.64	4.2	4.4	2.5	1.1	0.5	1.7	1.0	0.2		
1.68	3.5	4.0	2.1	1.0	0.5	1.4	0.8	0.2		
1.72	2.8	3.3	2.0	0.8	0.7	1.1	0.6	0.2	0.1	
1.76	2.3	2.8	1.6	0.7	0.4	0.8	0.4	0.1		
1.80	2.0	2.3	1.4	0.6	0.4	0.6	0.3	0.1		
1.84	1.8	2.1	1.5	0.6	0.5	0.4	0.3	0.1		
1.88	1.6	1.8	1.1	0.5	0.3	0.3	0.2	0.1		
1.92	1.2	1.4	0.9	0.4	0.2	0.2	0.2	0.1		
1.96	1.1	1.2	0.6	0.3	0.3	0.2	0.1			

Table 9. Normalization factors required to calculate the statistical error of the values given in Tables 1–8

Reaction	Energy (MeV/nucleon)	MUL1	MUL2	MUL3	MUL4	MUL5
Ca+Ca	400	971	1628	2135	1916	321
Nb+Nb	250	1564	754	502	343	62
Nb+Nb	400	714	359	263	165	9
Nb+Nb	650	174	101	75	60	6
Au+Au	250	1067	474	343	252	33
Au+Au	400	959	588	478	384	41
Au+Au	650	302	506	573	604	99
Ne+Au	2100	935	553	429	304	44

References

1. Gutbrod, H., Poskanzer, A.M., Ritter, H.G.: Rep. Proc. Phys. **52**, 1267 (1989)
2. Kampert, K.H.: J. Phys. G **15**, 691 (1989)
3. Aichelin, J., Stöcker, H.: Phys. Lett. B **176**, 14 (1986)
4. Aichelin, J., Peilert, G., Bohnet, A., Rosenhauer, A., Stöcker, H., Greiner, W.: Phys. Rev. C **37**, 2451 (1988)
5. Peilert, G.: Thesis, University of Frankfurt (1988) (unpublished)
6. Peilert, G., Rosenhauer, A., Aichelin, J., Stöcker, H., Greiner, W.: Mod. Phys. Lett. A **3**, 459 (1988)
7. Rosenhauer, Ph.D. Thesis, University of Frankfurt (1988)
8. Bohnet, A.: Thesis, University of Heidelberg (unpublished)
9. Ainsworth, T.L., Baron, E., Brown, G.E., Cooperstein, J., Prakash, M.: Nucl. Phys. A **464**, 740 (1987)
10. Aichelin, J., Rosenhauer, A., Peilert, G., Stöcker, H., Greiner, W.: Phys. Rev. Lett. **58**, 1926 (1987)
11. Bertsch, G.F., DasGupta, S.: Phys. Rep. **160**, 189 (1988)
12. Bertsch, G.F.: Phys. Rev. Lett. **34**, 697 (1975)
13. Berenguer, M.: Private communication (1989)
14. Baden, A., Gutbrod, H.H., Löhner, H., Maier, M.R., Poskanzer, A.M., Renner, T., Riedesel, H., Ritter, H.G., Spieler, H., Warwick, A., Weik, F., Wieman, H.: Nucl. Instrum. Methods **203**, 189 (1982)
15. Bertsch, G.F., Kruse, H., Das Gupta, S.: Phys. Rev. C **29**, 673 (1984)
16. Doss, K.G.R., Gustafsson, H.-Å., Gutbrod, H.H., Kolb, B., Löhner, H., Ludewigt, B., Poskanzer, A.M., Renner, T., Riedesel, H., Ritter, H.G., Warwick, A., Wieman, H.: Phys. Rev. C **32**, 116 (1985)
17. Doss, K.G.R., Gustafsson, H.-Å., Gutbrod, H.H., Kampert, K.-H., Kolb, B., Löhner, H., Ludewigt, B., Poskanzer, A.M., Ritter, H.G., Schmidt, H.R., Wieman, H.: Phys. Rev. Lett. **57**, 302 (1986)
18. Doss, K.G.R., Gustafsson, H.-Å, Gutbrod, H.H., Harris, J.W., Jacak, B.V., Kampert, K.H., Kolb, B., Poskanzer, A.M., Ritter, H.G., Schmidt, H.R., Teitelbaum, L., Tincknell, M., Weiss, S., Wieman, H.: Phys. Rev. Lett. **59**, 2720 (1987)
19. Doss, K.G.R., Gustafsson, H.-Å, Gutbrod, H.H., Hahn, D., Kampert, K.H., Kolb, B., Löhner, H., Poskanzer, A.M., Ritter, H.G., Schmidt, H.R., Stöcker, H.: Phys. Rev. C **37**, 163 (1988)
20. Doss, K.G.R., Gustafsson, H.Å., Gutbrod, H.H., Kampert, K.H., Kolb, B.W., Löhner, H., Ludewigt, B., Poskanzer, A.M., Ritter, H.G., Schmidt, H.R.: Mod. Phys. Lett. A **3**, 849 (1988)
21. Danielewicz, P., Odyniec, G.: Phys. Lett. **157** B, 146 (1985)
22. Fai, G., Randrup, J.: Nucl. Phys. A **404**, 551 (1983)
23. Fai, G., Randrup, J.: Comp. Nucl. Phys. Comm. **42**, 385 (1986)
24. Gustafsson, H.-Å., Gutbrod, H.H., Kolb, B., Löhner, H., Ludewigt, B., Poskanzer, A.M., Renner, T., Riedesel, H., Ritter, H.G., Warwick, A., Weik, F., Wieman, H.: Phys. Rev. Lett. **52**, 1590 (1984)
25. Gustafsson, H.-Å., Gutbrod, H.H., Kolb, B., Löhner, H., Ludewigt, B., Poskanzer, A.M., Renner, T., Riedesel, H., Ritter, H.G., Warwick, A., Wieman, H.: Phys. Lett. **142** B, 141 (1984)
26. Gutbrod, H., Kampert, K.H., Kolb, B.W., Poskanzer, A.M., Ritter, H.G., Schmidt, H.R.: Phys. Lett. B **216**, 267 (1989); Gutbrod, H., Kampert, K.H., Kolb, B.W., Poskanzer, A.M., Ritter, H.G., Schicker, R., Schmidt, H.R.: Phys. Rev. C (submitted)
27. Hartnack, C.: Thesis, University of Frankfurt (1989)
28. Hahn, D., Stöcker, H.: Nucl. Phys. A **476**, 718 (1988)
29. Molitoris, J.J., Stöcker, H.: Phys. Rev. C **32**, 346 (1985); Phys. Lett. B **162**, 47 (1985)
29. Kampert, K.H.: Ph. D. Thesis, University of Münster (1986) (unpublished)
30. Peilert, G., Stöcker, H., Greiner, W., Rosenhauer, A., Bohnet, A., Aichelin, J.: Phys. Rev. C **39**, 140 (1989)
31. Rosenhauer, A., Peilert, G., Stöcker, H., Greiner, W.: University of Frankfurt Preprint, UFTP 203/1987
32. Stöcker, H., Csernai, L.P., Graebner, G., Buchwald, G., Kruse, H., Cusson, R.Y., Maruhn, J.A., Greiner, W.: Phys. Rev. C **25**, 1873 (1982)
33. Stöcker, H., Greiner, W.: Phys. Rep. **137**, 277 (1986)
34. Schmidt, H.R., Gutbrod, H., Kampert, K.H., Kolb, B.W., Poskanzer, A.M., Ritter, H.G.: Proceedings of the Int. Workshop on Gross Properties of Nuclei and Nuclear Excitations XVII, Hirschegg (1989)
35. Stöcker, H., Hoffmann, J., Maruhn, J.A., Greiner, W.: Prog. Part. Nucl. Phys. **4**, 133 (1980)
36. Scheid, W., Müller, H., Greiner, W.: Phys. Rev. Lett. **32**, 741 (1974)
37. Sobel, M.I., Siemens, P.J., Bondorf, J.P., Bethe, H.A.: Nucl. Phys. A **251**, 502 (1975)
38. terHaar, B., Malfliet, R.: Phys. Rep. **149**, 207 (1987)
39. Welke, G.M., Prakash, M., Kuo, T.T.S., Das Gupta, S., Gale, C.: Phys. Rev. C **38**, 2101 (1988)

H.H. Gutbrod, B.W. Kolb, H.R. Schmidt
GSI
Postfach 110552
D-6100 Darmstadt 11
Federal Republic of Germany

A.M. Poskanzer, H.G. Ritter
Lawrence Berkeley Laboratory
Berkeley, CA 94720
USA

K.H. Kampert
Universität Münster
D-4400 Münster
Federal Republic of Germany